# Chapter 18

# Measuring In Vivo Protein Dynamics Throughout the Cell Cycle Using Microfluidics

**Roy de Leeuw, Peter Brazda, M. Charl Moolman, J.W.J. Kerssemakers, Belen Solano, and Nynke H. Dekker**

## Abstract

Studying the dynamics of intracellular processes and investigating the interaction of individual macromolecules in live cells is one of the main objectives of cell biology. These macromolecules move, assemble, disassemble, and reorganize themselves in distinct manners under specific physiological conditions throughout the cell cycle. Therefore, in vivo experimental methods that enable the study of individual molecules inside cells at controlled culturing conditions have proved to be powerful tools to obtain insights into the molecular roles of these macromolecules and how their individual behavior influence cell physiology. The importance of controlled experimental conditions is enhanced when the investigated phenomenon covers long time periods, or perhaps multiple cell cycles. An example is the detection and quantification of proteins during bacterial DNA replication. Wide-field microscopy combined with microfluidics is a suitable technique for this. During fluorescence experiments, microfluidics offer well-defined cellular orientation and immobilization, flow and medium interchangeability, and high-throughput long-term experimentation of cells. Here we present a protocol for the combined use of wide-field microscopy and microfluidics for the study of proteins of the *Escherichia coli* DNA replication process. We discuss the preparation and application of a microfluidic device, data acquisition steps, and image analysis procedures to determine the stoichiometry and dynamics of a replisome component throughout the cell cycle of live bacterial cells.

**Key words** Single-molecule techniques, Fluorescence imaging, Microfluidics, DNA replication, *Escherichia coli*

## 1 Introduction

Wide-field fluorescence imaging, based on conventional optical microscopy, can resolve structures in living cells down to approximately 200 nm, due to the diffraction limit of light. Although higher resolution microscopy techniques exist [1, 2], wide-field fluorescence imaging can still provide accurate information on the dynamics of single proteins inside living cells. Moreover, in combination with microfluidics it provides a reliable and statistically sound single-molecule method to observe the motion and

Olivier Espéli (ed.), *The Bacterial Nucleoid: Methods and Protocols*, Methods in Molecular Biology, vol. 1624,
DOI 10.1007/978-1-4939-7098-8_18, 

stoichiometry of individual proteins inside living cells [3]. To extract this information and subsequently gain insight into the ongoing biomolecular processes, obtained fluorescence images have to be treated with quantitative image analysis procedures.

To investigate dynamic processes during the cell cycle and obtain statistically relevant data it is essential that the environment for each studied cell is equivalent. Microfluidic devices are ideally suited for such studies with time-lapse fluorescence imaging, as they offer well-defined cellular orientation and immobilization, provide a constant flow and interchangeability of nutrients, and allow for high-throughput long-term experimentation of cells. The main advantage of using microfluidics compared to more conventional methods (e.g., the agarose gel [4]) is that, due to the uniform flow of nutrients, the cell's environment can be altered and set equivalent for every measured cell. This environment can also be modified homogeneously by changing the flow through the device (*see* **Note 1**).

This chapter describes the acquisition and post-processing analysis of wide-field fluorescence microscopy images obtained using a microfluidics device (*see* Fig. 1). First, the preparation of *Escherichia coli* (*E. coli)* cells from a genetically engineered strain is described. Second, the fabrication of a microfluidic device loaded with *E. coli* cells that can be readily used for fluorescence imaging is explained.

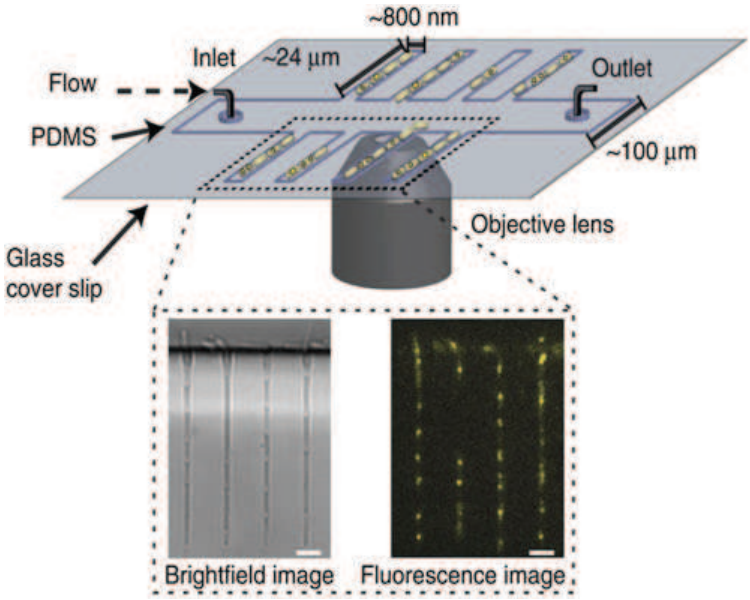


**Fig. 1** Wide-field microscopy with a cell-loaded microfluidic device. The microfluidic device used for performing long time-lapse fluorescence microscopy. *E. coli* cells are immobilized in growth channels perpendicular to a main trench through which growth medium is actively pumped. Fifteen channels are monitored in one field of view, with the channel height being 1 µm. The main trench height is ~15 µm. (*inset*) A brightfield image and corresponding YPet-$\beta_2$ fluorescence image (80 ms laser light exposure) are acquired every 2.5 min for the duration of the time-lapse experiment

Finally, the operation of the microscope and the custom-built image analysis procedures are discussed in detail.

This protocol is illustrated by using data of fluorescently labeled $\beta_2$-sliding clamps (DnaN), a DNA-binding protein with key functions in DNA replication in *E. coli*. They are used as markers to quantify the timing of the DNA replication cycle. A characteristic feature of the $\beta_2$-sliding clamp is that it remains DNA-bound during replication (high intensity signal) and diffuses freely when replication ceases (low intensity signal). This allows for the determination of the replication time by observing the evolution of the fluorescence intensity of spots within the cells over time. We recommend the use of the $\beta_2$-sliding clamp in addition to other proteins of interest so that processes can be accurately linked to the DNA replication cycle of the cell.

## 2 Materials

### 2.1 Microscope

Our optical setup is based on a customized commercial Nikon Ti-Eclipse microscope.

1. Commercial Nikon Ti-Eclipse microscope equipped with a Nikon CFI Apo TIRF 100×, 1.49NA oil immersion objective. The microscope is operated in epifluorescence (EPI) mode.
2. Electron Multiplying CCD (EMCCD) Andor iXon 897 camera operated by a personal computer (PC) running Nikon NIS-elements 4.20.01 software.
3. Cell outlines are imaged using the standard Nikon brightfield halogen lamp and condenser.
4. The fluorescence excitation is performed using an Omicron Laserage LightHUB containing a 514-nm laser.
5. The LightHUB is coupled into a single-mode optical fiber (KineFLEX) connected to the TI-TIRF-E arm input of the microscope.
6. The emission of the fluorescent proteins is projected onto the central part of the EMCCD camera using custom filter sets: Chroma Z514/10×, ET540/30 m, ZT514rdc-tirf (YPet 514 nm).
7. Custom design commercial temperature control housing (Okolabs) enclosing the microscope body.
8. Sample position controlled with a Nikon stage (TI-S-ER Motorized Stage Encoded, MEC56100) with the Nikon Perfect Focus System to eliminate Z-drift during image acquisition.

9. To synchronize camera shutter control with laser exposure, a National Instruments BNC-2115 connector block is used and controlled with NIS-elements.

### 2.2 PDMS Microfluidic Device Preparation

1. Sylgard 184 Silicone Elastomer Kit to make PDMS in various consistencies.
2. 1H,1H,2H,2H-perfluorodecyltrichlorosilane 97% to make PDMS mold hydrophobic.
3. VWR International 22 × 22 mm coverslips, Thickness No. 1 or 1.5, Cat. No. 631-0124, used for imaging the PDMS device.
4. HelixMark peristaltic pump tubing, Ref 60-825-27 for inlet and outlet.
5. BD 10 mL Syringe Luer-Lok Tip, Ref 300912. + BD Microlance 3 20G 1½″—Nr. 1, 0.9 × 40 mm, Ref 301300 to contain the medium.
6. F560088-90 dispensing needle, standard with thread. Rosa, ø 0.58 mm, 90°, ½″, to connect the tubes with the PDMS device.
7. Harris Uni-Core Multipurpose sampling tool, ø 0.75 mm to puncture holes in PDMS.
8. Harvard apparatus 11 plus syringe pump to control flow.
9. BSA Molecular Biology Grade. B9000S 20 mg/mL Lot: 0051502. Qty: 0.6 mL. Supplied in: 20 mM Tris–HCl, 100 mM KCl, 0.1 mM EDTA and 50% glycerol (pH 8.0 at 25 °C).
10. Customized Okolab Nikon Eclipse-Ti-E Cage Incubator.
11. Fisherbrand Falcon Tubes (50 mL), Cat. No. 06–443-18.
12. Eppendorf Centrifuge 5810R and an Eppendorf IL109 Carrier for the PDMS device.
13. Binder Classic Series B Incubator for PDMS heating.
14. Parafilm (Bemis Company, Inc.).
15. PDMS Mold obtained from Electron Beam Lithography (EBL) imprinted silicon wafer (*see* **Note 2**).
16. Oxygen Plasma-Preen I Barrel Reactor, Plasmatic Systems, Inc.

### 2.3 Strain and Culture Media

1. *E. coli* strain (YPet-$\beta_2$): a derivative of the *E. coli* K12 AB1157 strain.
2. Kanamycin dissolved in dH2O (50 mg/mL as stock solution, filter sterilized 0.22 μm).
3. M9-glycerol media: 1 L of M9 medium contains 10.5 g/L of autoclaved M9 broth (Sigma-Aldrich); 0.1 mM of autoclaved $CaCl_2$ (Sigma-Aldrich); 0.1 mM of autoclaved $MgSO_4$ (J.T. Baker); 0.3% of filter-sterilized glycerol (Sigma-Aldrich) as

carbon source; 0.1 g/L of filter-sterilized "5 amino acids" (L-threonine, L-leucine, L-proline, L-histidine, L-arginine (Sigma-Aldrich)), and 10 μL of 0.5% filter-sterilized thiamine (Sigma-Aldrich).

### 2.4 Data Analysis and Imaging Software

1. MATLAB (Mathworks, USA) is used for image processing procedures. The Image Processing Toolbox contains useful functions for image operations.
2. ImageJ 1.51a is used for image translation and rolling ball background correction.
3. NIS elements 4.20.01 is utilized to operate and configure the microscope.
4. The Omicron Laserage LightHUB Controller is used to control the laser power digitally.

## 3 Methods

### 3.1 Cell Culture

This section refers to the culturing of the YPet-$\beta_2$ strain *E. coli* strain (on AB1157 background). This strain is constructed by lambda-red recombination and has been thoroughly described (sequencing, cell morphology, doubling time) previously [3].

1. Inoculate a single colony of the YPet-$\beta_2$ strain from an LB-agarose plate (supplemented with the selection antibiotics, kanamycin (50 ng/mL)) and grow it in 5 mL M9-glycerol (supplemented with kanamycin (50 ng/mL)) overnight at 37 °C with 250 rpm shaking.
2. Initiate a secondary culture as a 1:500 dilution from the overnight culture in 5 mL M9-glycerol (supplemented with kanamycin) and incubate at 37 °C with 250 rpm shaking until OD600 0.1–0.3 is reached, to gain an exponential growth phase culture.
3. The secondary culture is used to load the microfluidic device in **step 13** of Subheading 3.2.

### 3.2 Preparation and Loading of the Microfluidic Device

1. Separate a single microfluidic device from a previously prepared PDMS array (*see* **Note 3**).
2. Place the freshly separated PDMS device into a glass petri dish.
3. Puncture holes at both ends of the main channel with a biopsy needle (this creates the complete main channel that is used to load the device and to provide the nutrient flow).
4. Clean a coverslip by exposing it to a flame, which is a fast and effective method for removing dirt particles from the glass (*see* **Note 4**).

5. Place a clean coverslip (side #1) next to the PDMS device in the glass petri dish.
6. Insert the glass petri dish with the microfluidic device and coverslip into the Plasma-Preen barrel reactor with the channels pointing upward, to activate both surfaces. Vacuum pump the barrel and flow oxygen gas into the chamber for ~10 s. Turn on the microwave at 800 W for 15 s to create oxygen plasma.
7. Flip the PDMS device onto the coverslip and press for full contact (*see* **Note 5**).
8. Heat the PDMS–coverslip construct (in the glass petri dish) for 10 min at 70 °C.
9. Cut roughly 30 cm of tubing for the inlet and outlet of the device. Remove the plastic handles of the two dispensing needles (*see* Subheading 2.2, **item 6**) and insert them in the inlet and outlet.
10. Fill a syringe with 12.5 mL mixture of M9-glycerol (with kanamycin (50 ng/mL)) and BSA (200 ng/mL). Remove air bubbles from the syringe. Insert the syringe needle into one tubing and remove the air by flushing some medium through the tube (*see* **Note 6**).
11. To prepare a mixture for BSA passivation of the PDMS device, add 100 μL of M9-glycerol to 100 μL of BSA in an Eppendorf tube. Create a 200 μL drop of the mixture in a petri dish. Soak up the drop slowly with the hook through the syringe, and avoid suction of air bubbles.
12. Insert the tubing at one end of the PDMS device (via one of the holes created at **step 3**) and slowly flush the channel with the 200 μL mixture, until a drop at the outlet appears (*see* **Note 7**). Keep a potential gradient by virtue of height of the syringe and wait for 45 min, to let the medium reach the end of every channel.
13. Take the second tubing and insert it in the outlet (the other hole, created at **step 3**) of the device. Pump medium through the device until medium appears at the outlet tubing. Disconnect the inlet from the device.
14. To prepare the cells for insertion, pellet 1 mL of the secondary culture by centrifugation (16100 × *g* for 1 min), wash it with 1 mL of fresh M9-glycerol and resuspend the culture in 80 μL M9-glycerol without antibiotics or BSA.
15. Make an 80 μL drop of culture on a petri dish and suck up the drop with the inlet hook connected to the syringe containing the medium. Inject 80 μL of this culture into the device by the inlet tubing until the culture suspension is observed at the outlet tubing. Remove the inlet and outlet tubings.

16. The device with the cells are centrifuged at 2500 × *g*, 15 °C for 10 min (ramp up 5, ramp down 5) to position the cells into the channels (*see* **Note 8**). One side of the PDMS device now contains channels with cells in them. The cells are then incubated for 30 min in the device with M9 drops on inlet and outlet, put within a petri dish containing a water drenched tissue.
17. After incubation, reconnect the inlet and outlet tubings to the device.

### 3.3 Microscopy

1. Set the temperature of the Okolab Cage to 37 °C.
2. Mount the PDMS device on the microscope. Install the syringe on the syringe pump (input of the device) and lead the outlet tubings coming from the PDMS device (output) into the waste container.
3. Bring the channels into focus with transient light illumination by using the eyepiece. Move the stage towards a position where at least three consecutive channels contain two to three cells (*see* **Note 9**, Fig. 2b). In a typical experiment 100–300 cells are recorded.
4. Remove debris and swimming cells from the main channel by turning on the syringe pump to flush the device at 10.5 mL/h. After the debris is removed, set the syringe pump to operative mode at 0.5 mL/h for the remaining experiment.
5. Turn on the EMCCD camera and set the electron multiplier gain (EM gain) to 0 for taking brightfield images and gain to 300 for taking fluorescence images.
6. Using NIS Acquisition in NIS elements, data acquisition is set to take a brightfield image and a fluorescence image with 80 ms exposure time every 150 s.
7. In the Omicron Control Center (OCC) the 514 nm laser is switched and the power is set to the equivalent of 5 W/cm$^2$ at the sample height (*see* **Note 10**).
8. The Perfect Focus System (PFS) is used during the measurement to ensure stability of focus along the optical axis during the experiment (*see* **Note 11**).

### 3.4 Analysis Protocols

1. Correct fluorescence images for nonuniformity by dividing the images with the normalized laser beam image, in ImageJ (*see* Fig. 2). Laser illumination of the sample is nonuniform, due to the Gaussian irradiation profile of the laser beam.
2. Perform rolling ball background subtraction to remove background from the image and to isolate bright spots using the rolling ball background subtraction algorithm in ImageJ, with a rolling ball radius of 10 pixels (0.159 μm/px).

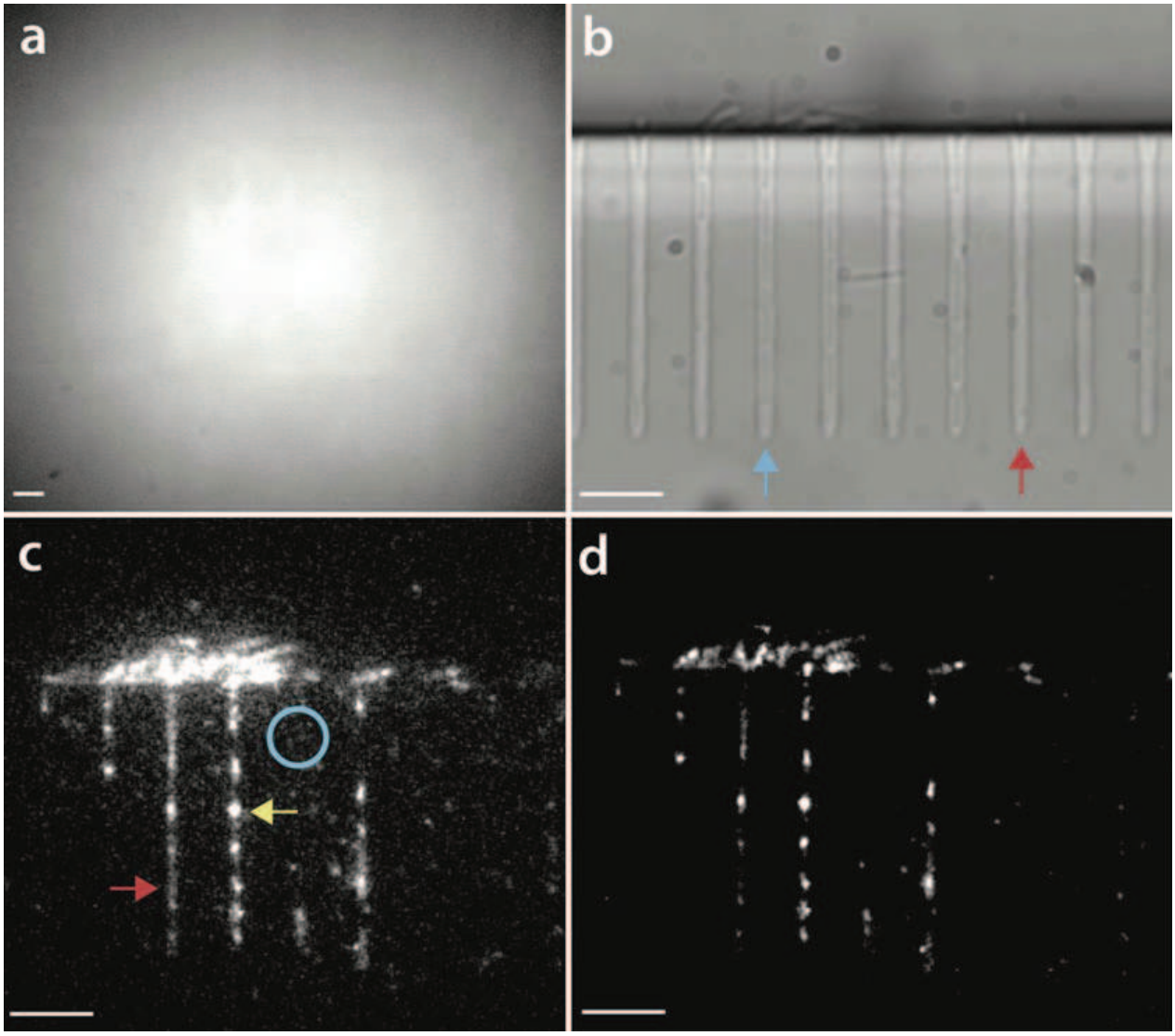


**Fig. 2** Examples of images relevant to fluorescence image correction**.** (**a**) Beam profile of 514 nm laser illumination on an autofluorescent plastic slide (Chroma). *Dark areas* can be observed at the corners of the image, showing its Gaussian illumination profile. (**b**) Brightfield image of the microfluidic device loaded with cells, where the *red arrow* indicates an empty channel, and the *blue arrow* shows a cell-filled channel. (**c**) The raw fluorescence image of the device shown in **b** being illuminated by a 514-nm laser. The *blue area* indicates a region of high background noise, the *yellow arrow* shows a cell with a bright fluorescent spot (actively replicating) and the *red arrow* shows a cell emitting a low uniform intensity (nonreplicating). (**d**) Image **c** with corrected background and laser illumination. The background noise is reduced and the fluorescent spots are clearly visible, including ones on the periphery of the image. *Scale bars* mark 5 μm

3. Align the fluorescence and brightfield images using an X–Y image translation algorithm in ImageJ. The required translation is obtained by performing a calibration measurement with fluorescent beads, 0.5 μm in diameter (*see* **Note 12**).
4. To determine the X–Y drift of the sample during the measurement (*see* Fig. 2d) a high-contrast region is tracked over the time interval of the experiment. Select a high-contrast region of interest (ROI) (e.g., dirt particle or channel edge) within the

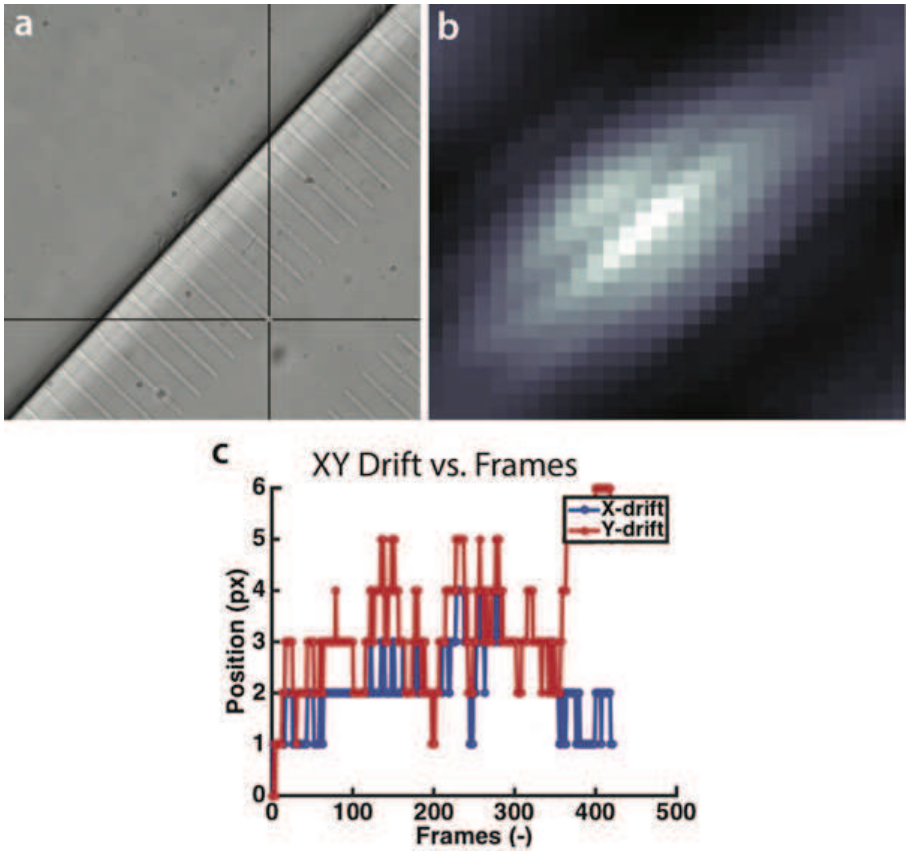


**Fig. 3** Determining the drift of the microfluidic device during the time-lapse experiment. (**a**) A high-contrast region of interest (ROI) is selected (*see black crosshair*) in the first brightfield image of the microfluidic device to determine the drift of the sample during the experiment. (**b**) The cross-correlation plot of the ROI compared to the initial ROI image, where the highest intensity value position denotes the shift in position. (**c**) Graph of the resulting translation in *X* and *Y* (in pixels) during the captured frames of the time-lapse measurement. The negatives of the *X* and *Y* in these plots are imposed as translation to the images to counter drift

first image (*see* Fig. 3a). Track the motion of the ROI by using image cross-correlation of the ROI images with the first ROI image (*see* Fig. 3b). Use the resulting X–Y translation vectors (*see* Fig. 3c) to translate the image series correspondingly to stabilize the images.

5. Select the microfluidic channels that are chosen for analysis (*see* **Note 9**) by using a custom made clicking algorithm on a brightfield sample image (Fig. 4a). Clicking parameters (e.g., channel length, channel angle, number of channels, and distance between channels) are specified such that one click is required to select multiple channels. This algorithm makes new time-lapses of individual channels.
6. Generate kymographs for the selected microfluidic channels, for brightfield and fluorescence data (*see* Fig. 4b). The

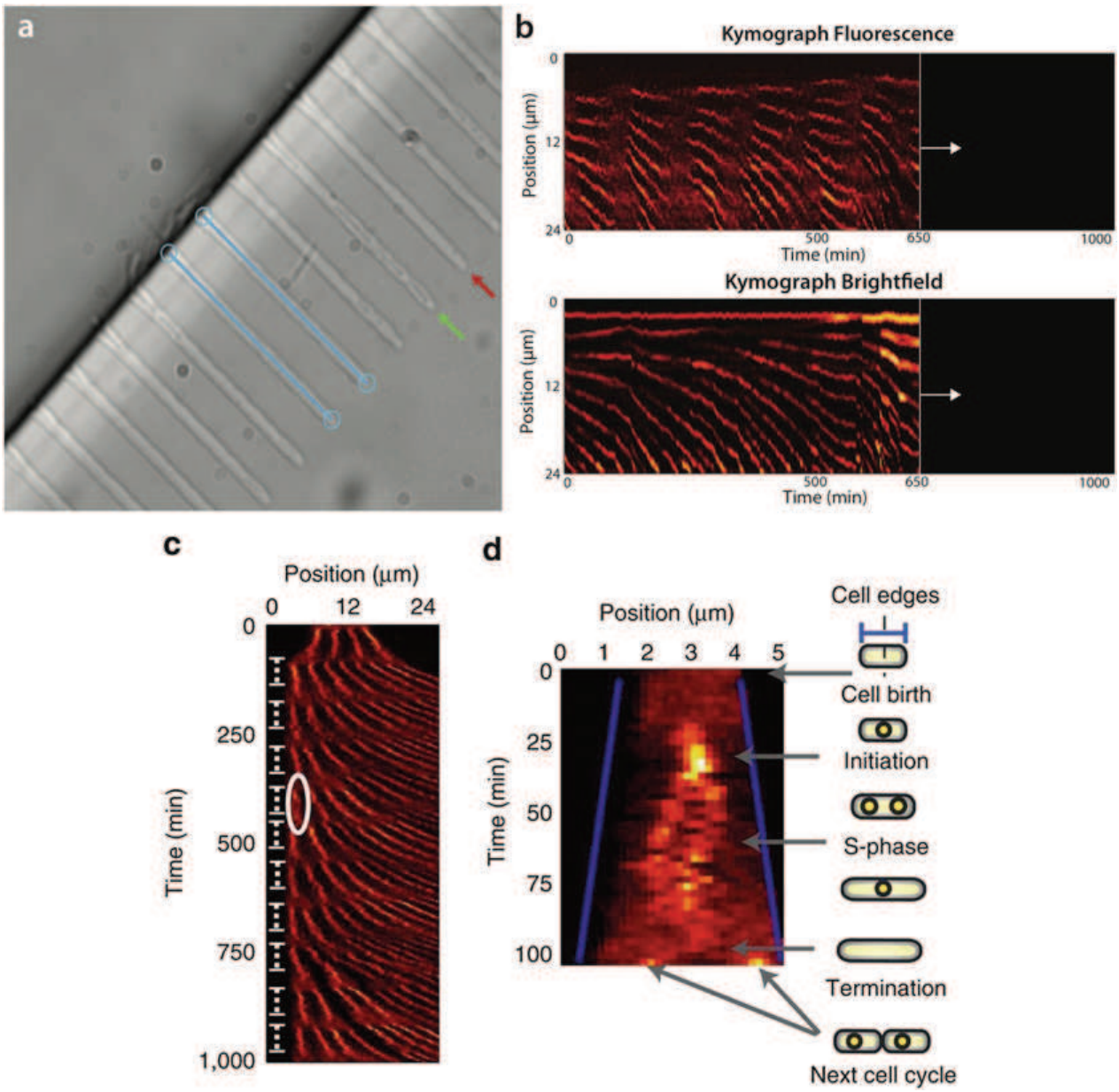


**Fig. 4** (**a**) A sample brightfield image of the microfluidic device is used to manually select the channels to make kymographs from. After the user has clicked on the microfluidic channel, *blue lines* show the selection, such that the user can evaluate whether selection is accurately along the channel. A channel containing cells (*green*) and an empty channel (*red*) are indicated by *arrows*. (**b**) Progression of the generation of a fluorescence and brightfield kymograph for one microfluidic channel. The kymograph image is constructed by combining small image strips of the selected microfluidic channel over all time points. In this example the graph is truncated at the image strip corresponding to the 650th minute to show the progressive nature in constructing the kymograph. The curvature of the fluorescence signal is due to the individual cells growing and pushing each other in the direction of the main trench. (**c**) Kymograph of a single growth channel during a time-lapse experiment. Clearly observable diffuse patterns occur at regular intervals, indicating the lack of DNA-bound $\beta_2$-clamps before initiation and after termination. The repeating pattern is due to the multiple cycles of replication. Each replication cycle is indicated with a *vertical dashed line* on the *left-hand side* of the image. The *white ellipsoid* indicates an individual replication cycle. (**d**) The detailed kymograph of an individual replication cycle indicated by the *ellipsoid* in **c**. The *blue lines* are the cell boundaries detected from the brightfield field images. The illustrations on the *right-hand side* indicate the different stages of replication that take place during the cell cycle, with *grey arrows* pointing toward the position in the fluorescent data

kymograph image is constructed by combining small image strips of the selected microfluidic channel over all time points. These graphs provide spatial and temporal information of the cell sizes (cell poles) and proteins (fluorescent clusters). The fluorescence kymograph is created by using the corrected fluorescent images, while the brightfield kymograph is constructed by differentiated brightfield images with respect to the direction of the channel. The differentiation is done such that high contrast gradients (space between neighboring cell poles) will show spot-like intensities. Use the differentiated images containing these spots to create the brightfield kymograph.

7. The kymographs allow a high-throughput manual clicking procedure to follow the replication cycle of the cells. Click on the kymograph to select the initiation of replication for the first cells, the first top image strip which has a spot (*see* Fig. 4c, d, replication initiation). Do this step first on a zoomed-in part of the starting section of the kymograph (*see* white circles in Fig. 5a). A larger fraction of the kymograph is then displayed. Click the end of the observed fluorescent spots. Connect these dots to two reappearing fluorescent spots below the termination point (*see* lower white dots in Fig. 5b). This denotes the initiation of the replication cycle of the two daughter cells (*see* Fig. 5b). Click in this manner through every generation.

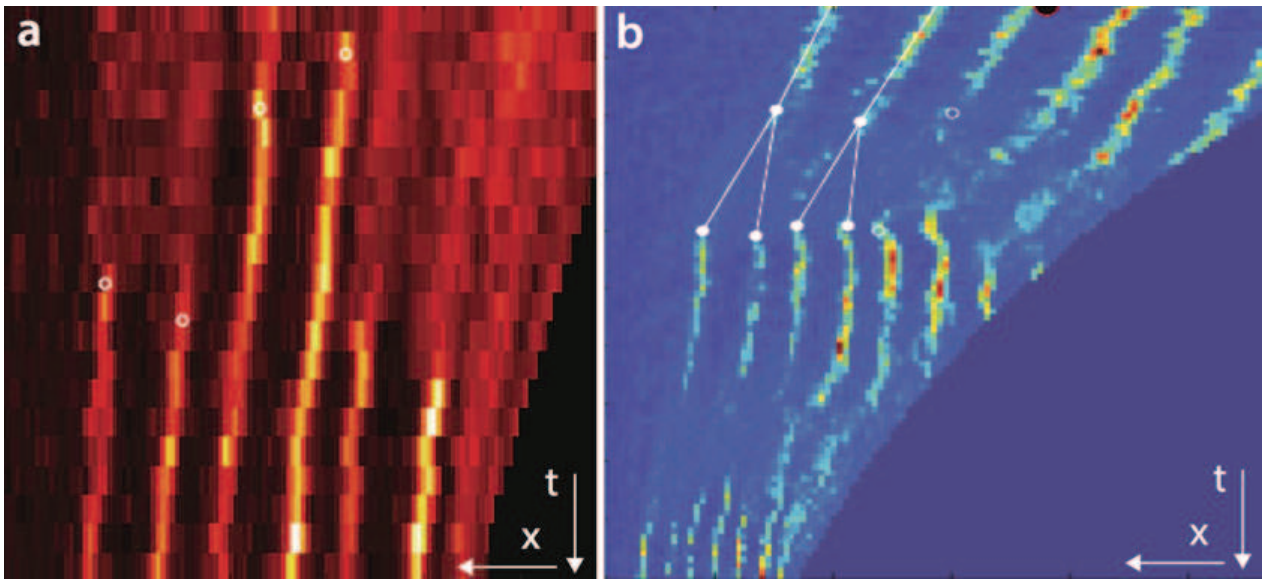


**Fig. 5** The kymograph replication cluster clicking procedure**.** (**a**) A zoomed image of the start of the kymograph is used to click (*white circles*) the beginning of measured fluorescent spots (*bright lines*), indicating the beginning of replication for each cell. (**b**) A larger fraction of the kymograph displayed to click the end of the observed fluorescent spots (replication ceases here), and to connect it to the two reappearing fluorescent spots as the daughter cells start their own replication cycle. Replication profiles are curved in the kymograph as a result of cell growth. This is corrected for to facilitate the user clicking process. The color maps are chosen in such a way that the user can better recognize the cycle events

Different zooms on the kymograph help to complete this procedure for the full time-lapse experiment.

8. Use the clicks created in **step 6** and the brightfield kymograph to determine the replication and division time (*see* Fig. 6a). The division is determined by the appearance of new cell poles in the brightfield kymograph (*see* **Note 13**). The replication time is determined by the distance between the clicks on the fluorescence kymograph. Set intensity thresholds according to the individual intensity value of the protein of interest.

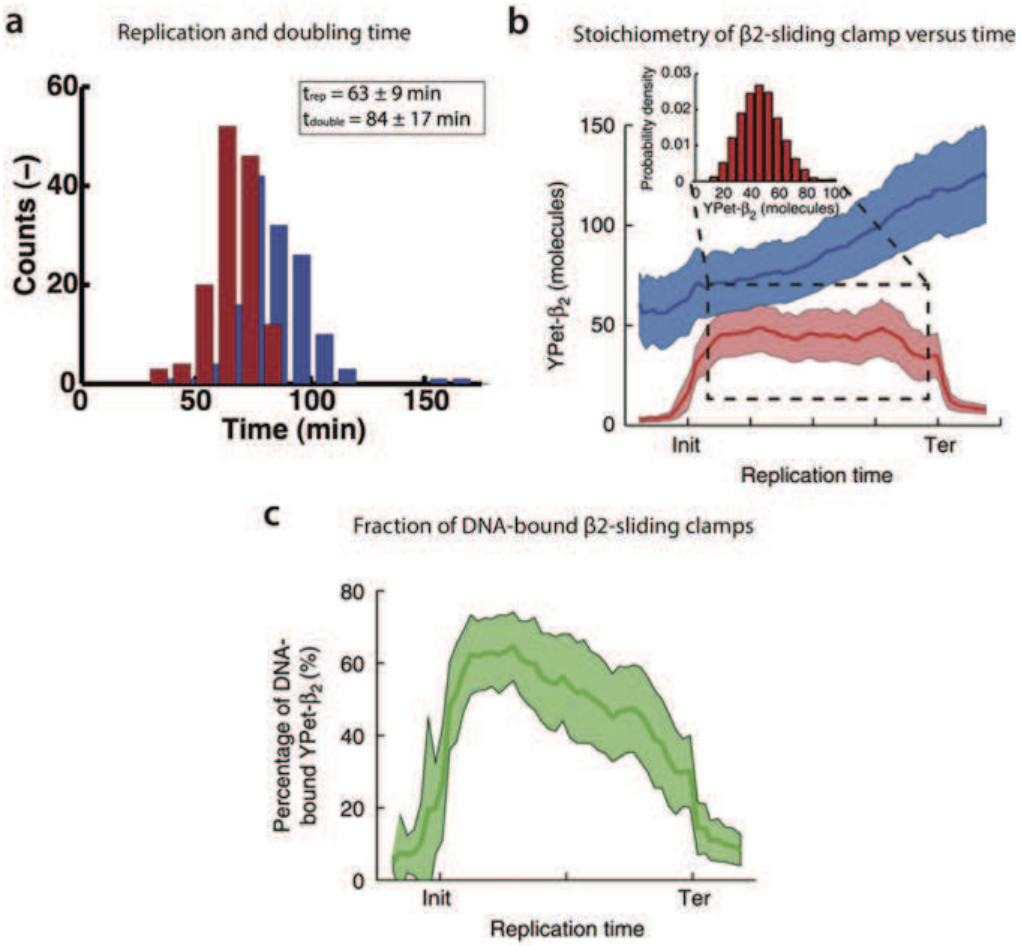


**Fig. 6** Quantification of the in vivo $\beta_2$-sliding clamp stoichiometry during replication**.** (**a**) The division ($t_{double}$, *blue*) and replication ($t_{rep}$, *red*) time distributions of the YPet-$\beta_2$ *E. coli* strain in the microfluidic device during a long time-lapse experiment. (**b**) The YPet–$\beta_2$ molecules in the whole cell (*blue curve*) approximately double during the cell cycle, from 60 to 120 YPet–$\beta_2$ molecules. The DNA-bound YPet–$\beta_2$ molecules (*red curve*) remarkably increase to a mean steady state value of 46 YPet–$\beta_2$ molecules following initiation. (*inset*) A histogram of the distribution of number of DNA-bound YPet–$\beta_2$ molecules during steady state. (**c**) The fraction of DNA-bound YPet–$\beta_2$ molecules varies over the course of the replication cycle. At the midway point of the replication cycle (indicated by a *tick mark*), this fraction equals 45%

9. The output of **step 7** also includes data of nonreplicating or nongrowing cells, so a set of criteria (fluorescence intensity, cell size, and cell cycle time thresholds) is implemented to ensure that the analysis is done only on actively replicating cells.
10. Generate individual cell time-lapse datasets, containing fluorescence image data of single cells, by using the cell pole data from the brightfield kymograph to crop fluorescent images from pole to pole.
11. Apply bleaching correction by measuring the fluorescence intensity per cell length for the individual cells. Correct the fluorescence images for the factor by which the intensity drops during the cell cycle of the cell, to properly account for the bleached molecules (*see* **Note 14**).
12. Analyze the cell time-lapse datasets in terms of spot intensity (stoichiometry, *see* **Note 15**) and the total fluorescence intensity coming from the cell. The spot intensity is properly accounted for by fitting a 2D Gaussian to the spot data, and a weighted integration is done over the area to get the integrated intensity. By knowing the integrated intensity coming from one of the utilized fluorescent proteins, the molecules can then be counted on the observed spot (*see* Fig. 6b). Determine the total cell intensity by summing the intensity of the pixels that make up the cell. After this step it is possible to plot the fraction of molecules in the spot (DNA-bound) versus all the molecules in the cell (DNA-bound and freely diffusing in the cytoplasm, *see* Fig. 6c).

## 4 Notes

1. There are several alternative and combined applications of the methods for microfluidics [5].
2. If you do not have access to clean room facilities able to do EBL, PDMS molds can be obtained from external sources [6]. Make sure to store the microfluidic channels facing upward (not to damage the protruding details) in a closed container (to protect it from dust contamination).
3. The PDMS array is obtained from a PDMS mold as described previously in detail [7]. PDMS is mixed in a 1:10 ratio, degassed, and poured onto the previously cured PDMS mold. After another degassing step, the device is allowed to cure for 2 h at 85 °C. Once the curing is complete, the PDMS is left to cool down for at least 30 min. Subsequently, the two PDMS layers (the mold and the actual device) are separated from each other. At this point the PDMS mold can be stored for later use.

4. Optionally, sonication can be applied for cleaning the cover glasses; Put the cover glasses in a holder that is submerges into a beaker. Place the beaker into a sonicator (Branson Ultrasonics B1510, USA). Apply 15 min of sonication in acetone (Sigma-Aldrich), then 15 min in isopropanol (Sigma-Aldrich), followed by a 15-min sonication in $dH_2O$. Blow-dry the cover glasses then with $N_2$ gas.
5. When attaching the PDMS device to the coverslip, make sure to use the plasma-activated surface of the glass that is facing upward during the oxygen plasma step. Apply some pressure on the PDMS device on the glass to obtain full contact of the surfaces.
6. Before inserting the syringe needle into the tubing, make sure that air bubbles are removed. This is best done by holding the tip upward and tapping it until the bubbles travel close to the tip. Press the end of the syringe until the air is removed.
7. Make sure that you do not introduce air into the device when injecting the M9–BSA mixture.
8. Before centrifuging the cells into the channels, put M9 drops on inlet and outlet to prevent the device to dry. On the coverslip, indicate the direction of centrifugation so that you know what side of the device contains channels with cells.
9. The channels chosen for analysis are the ones that contain more than three cells initially. Cells might stay close to each other even though they are physically separated. This prevents us from detecting the brightfield "spot" in the differentiated brightfield image. However, one could still use the fluorescence images and the clicks generated from the kymographs for determining the division time. As we use minimal medium, initiation of replication in a daughter cell occurs after the cell has divided. Between replication profiles cell division must have taken place. If we are unable to track a new pole between replication cycles, we estimate it to be in the middle of that time interval.
10. The required laser power to reach a specific intensity at the sample height varies from setup to setup [8].
11. Make sure that the Perfect Focus System (PFS) offset is set into the NIS acquisition configuration with command: PFS_define_offset(*offset_value*) (NIS elements). Determine a good offset by looking live at the sample while being laser illuminated, and change the offset such that the fluorescent spots are in focus and the image is sharp.
12. Determine the center position of fluorescent beads (TetraSpeck Fluorescent Microspheres Size Kit, Molecular Probes) for fluorescence images, by fitting a 2D Gaussian function over

the spot profile. The center position in the brightfield image is determined by inverting the image (such that it appears as a light spot) and fitting a 2D Gaussian function over the spot profile. The deviation between the center positions determines the required translation between the fluorescence and brightfield images.

13. It is recommended to judge by eye which channels are best fit for analysis, prior to the experiment. Criteria can be the number of cells in the channel (ideally it should be filled), the fluorescence activity of the cells (a filled channel can contain nonliving cells), the physiological state of the cells (deformed shape and size), or the quality of the channel shape itself (channel can be too wide, judged by mobility of cells within).
14. To correct for photobleaching, we use the following approach. We assume that cell growth and protein copy number in the cell increases linearly from cell birth until cell division. The ratio of these two numbers, as function of time, should remain constant throughout the cell cycle of a cell if there is no photobleaching. However, due to photobleaching, this ratio will decrease as function of time. We fit this curve with a single exponential and multiply the detected fluorescent signal with the appropriate factor as function of time in order to correct for this decline in fluorescence due to photobleaching.
15. To determine the stoichiometry of the spots, one has to know how many photons are excited from the single fluorophore that is used to label the protein. An additional calibration measurement is therefore required to determine the integrated intensity of the spot resulting from a single fluorescent protein. This can be an in vivo photobleaching experiment [9] or an in vitro single-molecule photobleaching assay [10].

## Acknowledgments

The authors would like to thank the members of the Nynke H. Dekker laboratory for discussions on the chapter. We thank Sriram T. Krishnan for his active involvement in the experiments discussed here, Jacob W.J. Kerssemakers for contributing to the development of the data analysis procedures, and Margreet Doctor for building and maintaining the experimental setup. The experiments described here were carried out in the Department of Bionanoscience, Delft University of Technology.

## References


1. Huang B, Bates M, Zhuang X (2009) Super-resolution fluorescence microscopy. Annu Rev Biochem 78(1):993–1016. doi:10.1146/annurev.biochem.77.061906.092014
2. Schermelleh L, Heintzmann R, Leonhardt H (2010) A guide to super-resolution fluorescence microscopy. J Cell Biol 190 (2):165–175. doi:10.1083/jcb.201002018
3. Moolman MC, Krishnan ST, Kerssemakers JWJ, van den Berg A, Tulinski P, Depken M et al (2014) Slow unloading leads to DNA-bound ß2-sliding clamp accumulation in live Escherichia coli cells. Nat Commun 5:5820. doi:10.1038/ncomms6820
4. Joyce G, Robertson BD, Williams KJ (2011) A modified agar pad method for mycobacterial live-cell imaging. BMC Res Notes 4:73. doi:10.1186/1756-0500-4-73
5. Sia SK, Whitesides GM (2003) Microfluidic devices fabricated in poly(dimethylsiloxane) for biological studies. Electrophoresis 24(21): 3563–3576. doi:10.1002/elps.200305584
6. Microfluidic foundry company website: http://www.microfluidicfoundry.com/moldpdms.html
7. Moolman MC, Dekker NH, Kerssemakers JWJ, Krishnan ST, Huang Z (2013) Electron beam fabrication of a microfluidic device for studying submicron-scale bacteria. J Nanobiotechnol 11:1–10
8. Grünwald D, Shenoy SM, Burke S, Singer RH (2008) Calibrating excitation light fluxes for quantitative light microscopy in cell biology. Nat Protoc 3(11):1809–1814. doi:10.1038/nprot.2008.180
9. Hines KE (2013) Inferring subunit stoichiometry from single-molecule photobleaching. J Gen Physiol 141(6):737–746. doi:10.1085/jgp.201310988
10. Reyes-Lamothe R, Sherratt DJ, Leake MC (2010) Stoichiometry and architecture of active DNA replication machinery in *Escherichia coli*. Science 328:498–501